J. Biomechanics Vol. 25, No. 3, pp. 223–234, 1992.
Printed in Great Britain

0021-9290/92 $5.00+.00
Pergamon Press plc

MECHANICAL ANALYSIS OF THE LANDING PHASE IN HEEL–TOE RUNNING

MAARTEN F. BOBBERT, MAURICE R. YEADON and BENNO M. NIGG
Human Performance Laboratory, Faculty of Physical Education, University of Calgary, Canada

Abstract—Results of mechanical analyses of running may be helpful in the search for the etiology of running injuries. In this study a mechanical analysis was made of the landing phase of three trained heel–toe runners, running at their preferred speed and style. The body was modeled as a system of seven linked rigid segments, and the positions of markers defining these segments were monitored using 200 Hz video analysis. Information about the ground reaction force vector was collected using a force plate. Segment kinematics were combined with ground reaction force data for calculation of the net intersegmental forces and moments.

The vertical component of the ground reaction force vector F_z was found to reach a first peak approximately 25 ms after touch-down. This peak occurs because, in the support leg, the vertical acceleration of the knee joint is not reduced relative to that of the ankle joint by rotation of the lower leg, so that the support leg segments collide with the floor. Rotation of the support upper leg, however, reduces the vertical acceleration of the hip joint relative to that of the knee joint, and thereby plays an important role in limiting the vertical forces during the first 40 ms. Between 40 and 100 ms after touch-down, the vertical forces are mainly limited by rotation of the support lower leg.

At the instant that F_z reaches its first peak, net moments about ankle, knee and hip joints of the support leg are virtually zero. The net moment about the knee joint changed from −100 Nm (flexion) at touch-down to +200 Nm (extension) 50 ms after touch-down. These changes are too rapid to be explained by variations in the muscle activation levels and were ascribed to spring-like behavior of pre-activated knee flexor and knee extensor muscles. These results imply that the runners investigated had no opportunity to control the rotations of body segments during the first part of the contact phase, other than by selecting a certain geometry of the body and muscular (co-)activation levels prior to touch-down.

INTRODUCTION

The increase in the number of people who run in order to improve their physical fitness has been accompanied by an increase in the prevalence of musculoskeletal injuries due to running. Most of these injuries are classified by clinicians as 'overuse injuries'. In biomechanical terms the development of an overuse injury to an anatomical structure may be formulated as follows. During each running step, the stress developed within the structure is so high that biological reactions take place which, in the long term, reduce the maximal stress that can be sustained without failure. When this maximal stress drops below the stress actually encountered during running, microtraumata or macrotraumata occur, which constitute an injury.

In the search for the etiology of overuse running injuries and methods of prevention, it would be ideal if time histories of stresses within structures could be determined during running and compared among injured and noninjured individuals, preferably in prospective epidemiological studies. Unfortunately, this is a utopian situation; it is currently impossible to measure stresses *in vivo*, and in order to calculate stresses we have to make so many assumptions that even the order of magnitude of the outcome is questionable. A crucial unknown in the calculation of stresses is, for instance, how the total force acting on an anatomical structure is distributed over the cross-sectional area of the structure. The only information that can be obtained reliably and routinely seems to consist of measured kinematics and ground reaction forces, and calculated net intersegmental forces and moments. Given the fact that these variables are indirectly related to stresses in anatomical structures, they may bear some relationship to running injuries. The only way to find out whether such a relationship exists is to conduct an epidemiological study in which time histories of the variables are compared among injured and noninjured runners. If differences are found, it may be useful in the search for methods of preventing injuries to compare the variables under various experimental conditions. In this case, varying shoe construction could be an important means of creating different experimental conditions since the choice of footwear is probably all that can be influenced in recreational runners.

It seems reasonable to assume that some running injuries are related to phenomena that occur during the landing phase of a running stride. In this phase, the muscles involved in reducing the momentum of body segments are forcibly lengthened, which could cause them to develop large stresses. Also in this phase, runners who strike the ground first with their rearfoot

Received in final form 11 *July* 1991.

Address correspondence to: Maarten F. Bobbert, Vrije Universiteit, Vakgroep Functionele Anatomie, Faculteit der Bewegingswetenschappen, v.d. Boechorststraat 9, 1081 BT Amsterdam, The Netherlands.

produce an 'impact force peak': a high-frequency peak in the time history of the vertical ground reaction force (F_z) during the first 50 ms of ground contact (Cavanagh and LaFortune, 1980; Frederick *et al.*, 1981; Nigg *et al.*, 1987). These force peaks may be accompanied by high stresses on bones and joint surfaces. Information about ground reaction forces during the landing phase in running is already available in the literature (e.g. Cavanagh and Lafortune, 1980), and the extent to which the magnitude of ground reaction force peaks depends on the properties of running shoes has also been studied (Lees and McCullagh, 1984; Komi *et al.*, 1987; Nigg and Morlock, 1987; Nigg *et al.*, 1987, 1988). However, a mechanical analysis of the landing phase in running, which is needed to improve our understanding of muscle functioning during this phase, has not been made. A crucial question is whether positional data of sufficient accuracy can be obtained for a mechanical analysis: the high-frequency peaks in $F_z(t)$ reflect high-frequency acceleration peaks of body segments, and these acceleration peaks have to be reconstructed by double differentiation of marker position time histories. In a previous study (Bobbert *et al.*, 1991) the first force peak in $F_z(t)$ during heel–toe running could be reconstructed with errors less than 10% from positional data, suggesting that the method of collecting and processing these data is sufficiently accurate to be used for a mechanical analysis. The purpose of the present study is to make such a mechanical analysis of the landing phase in heel–toe running, with a focus on the role of segmental rotations in limiting the forces which occur during this phase, and the role of muscle moments in controlling segmental rotations.

METHODS

Subjects and experimental protocol

Three trained male 10 km runners (times ranging from 33 to 38 min) participated in this study. Their characteristics (mean ± standard deviation) were: age 28 ± 4 yr, height 1.82 ± 0.03 m, body mass 71 ± 4 kg. Retroreflective spheres were applied to their bodies in order to define seven body segments: the two feet, the two lower legs, the two upper legs, and one segment comprising head, arms and trunk (HAT). The arms were not incorporated separately; in pilot work it had been established that they do not affect F_z to a significant extent in the early support phase (see also Bobbert *et al.*, 1991; Hinrichs *et al.*, 1987). The subjects were instructed to run along a 30 m runway, in the middle of which a force plate was mounted. Each subject performed five running trials in which he was allowed to use his preferred speed and style. Subsequently, running speed and running style were varied across a number of additional trials so as to obtain a wide range in orientations and velocities of body segments at touch-down. One of the subjects performed 15 additional trials, the other two subjects each performed only five additional trials. For each trial the subject adjusted the length of the approach until he landed consistently with his right foot on the force plate. During running, the force plate was used to determine the three orthogonal components and the point of application of the ground reaction force vector, and a high-speed video analysis system was used to monitor the 3-D positions of the retroreflective spheres. For the kinematic analysis, linear and angular displacements, velocities and accelerations of the body segments were calculated from the positional data. Net intersegmental forces and moments were calculated using an inverse dynamics approach, combining kinematic information, the measured ground reaction force vector and its point of application, and values reported in the literature for locations of segmental mass centers, segmental masses and segmental moments of inertia. Methods and procedures are detailed below. For reasons of conciseness, only results of the analysis in the sagittal plane projection will be presented.

Collection and processing of ground reaction force data

The three orthogonal components and the point of application of the ground reaction force vector were determined using a force plate (KISTLER type 9287, Kistler Instrumente AG, Winterthur, Switzerland), which was installed according to the manufacturer's specifications. The force plate was connected to an electronic amplifier unit (KISTLER type 9861A, Kistler Instrumente AG, Winterthur, Switzerland), and the eight output signals of this unit were sampled at 1000 Hz using a data acquisition board (DT2821-F-16SE, Data Translation Inc., Marlborough, MA) and a personal computer (COMPAQ Portable III, Compaq Computer Corp., Houston, TX). The x, y and z components of the ground reaction force vector, and the x and y coordinates of its point of application, were calculated using standard equations supplied by the manufacturer (Kistler, 1984). The accuracy of the calculated point of force application was subsequently improved using the algorithm developed by Bobbert and Schamhardt (1990), which corrects for symmetrically distributed errors found in a systematic comparison of calculated and known points of force application.

For the purpose of synchronization of force plate and video data, the analog F_z output of the amplifier unit was fed to an electronic circuit including a light-emitting diode (LED) in view of one of the video cameras. The threshold in the circuit was such that the LED came on when F_z exceeded 20 N.

Collection and processing of posititional data

The method of collecting video data has been detailed elsewhere (Bobbert *et al.*, 1991), and will be described only briefly below. In order to minimize the amount of skin movement relative to the mass center of leg segments, a device was used on each leg. The

device consisted of two light wooden rods connected by a hinge joint. The hinge joint was aligned with the estimated flexion–extension axis of the knee joint (at the height of the lateral collateral ligament, 2 cm above the tibial plateau). Subsequently, one rod was fastened to the lower leg and one to the upper leg using athletic tape and elastic bandages. Retroreflective spheres with a diameter of 2 cm were fixed to the wooden rods at the height of the estimated plantarflexion/dorsiflexion axis of the ankle joint (on the lateral malleolus, 0.5 cm anterior to its tip), the axis of the hinge joint, and the estimated axis of flexion/extension of the hip joint (2 cm proximal to the greater trochanter). Two retroreflective markers were also applied to the lateral side of the shoe of the support leg, one at the height of the 5th metatarsophalangeal joint, the other at the height of the tuber calcanei. On the upper body, one marker was taped to the skin at the height of the sternum (with long strips of athtletic tape running from below the sternum diagonally across the thorax, over the neck, to the shoulder blades) and one marker was fixed on top of the head (using an elastic band passing under the chin). The latter two markers were retroreflective spheres with diameters of 4 cm. The marker positions are shown schematically in Fig. 1.

Video data were collected using a VP310 video recorder (Motion Analysis Corporation, Santa Rosa, CA) and four electronically shuttered cameras (NAC MOS V-14 Camera 60/220 F/S) equipped with 12–120 mm zoom lenses (Angénieux, Paris, France). A 1000 W lamp was placed directly behind each camera. The cameras were zoomed in to a volume of 2 m in the x direction (axis along which subjects were running), 1 m in the y (medio-lateral) direction and 2 m in the z (vertical) direction, with the center of the base area corresponding to the center of the force plate. This volume was subsequently calibrated using 16 control points and Expert Vision 3-D software.

During running, data were collected at 200 Hz, the maximum sampling frequency of the system. For synchronization of video data with force data, the LED described above was used. The first video frame on which it was detected was taken to correspond in time to the second force sample following the one where F_z had exceeded the 20 N threshold. This way, synchronization errors ranged from -3 to $+2$ ms.

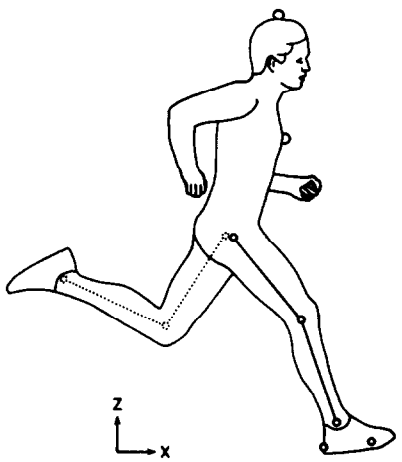

Fig. 1. Locations of markers used to define the position of body segments.

Time histories of marker positions were determined using Expert Vision 3-D software and smoothed using a Butterworth 4th order (zero lag) filter. A cutoff frequency of 15 Hz was used for smoothing position time histories of head and sternum markers, 50 Hz was used for all other markers. In a previous study (Bobbert *et al.*, 1991) it has been shown that lowering the cutoff frequency for head and sternum markers from 50 to 15 Hz resulted in a slight improvement during the landing phase of the correspondence between $F_z(t)$ calculated from positional data and $F_z(t)$ measured using a force plate. The smoothed position time histories were differentiated numerically using a direct 3-point derivative routine in order to obtain time histories of linear velocities and accelerations. Angles of body segments with the horizontal were calculated from the smoothed marker position time histories, and differentiated to obtain time histories of angular velocities and accelerations.

Kinematic analysis

The kinematic data were used to produce stick figures in which the linear velocity and acceleration vectors of markers were displayed as a function of position. As mentioned before, only results of the analysis in the sagittal plane (projection on x–z plane) will be presented. The difference in the vertical accelerations of the knee and the ankle joint markers ($\ddot{z}_K - \ddot{z}_A$) was analyzed as follows. The vertical distance between the knee and the ankle joint markers ($z_K - z_A$) is given by

$$(z_K - z_A) = l_1 \sin\theta_1, \tag{1}$$

where l_1 is the length of the line segment defined by the two markers (length of the lower leg), and θ_1 is the angle between this line segment and the horizontal. Double differentiation of both sides of equation (1) with respect to time yields

$$(\ddot{z}_K - \ddot{z}_A) = l_1\ddot{\theta}_1 \cos\theta_1 - l_1\dot{\theta}_1^2 \sin\theta_1 + \ddot{l}_1 \sin\theta_1 + 2\dot{l}_1\dot{\theta}_1 \cos\theta_1. \tag{2}$$

If l_1 is taken to represent the length of the bones of the lower leg, it should remain virtually constant and all the terms including the derivatives of l_1 should be negligible, giving

$$(\ddot{z}_K - \ddot{z}_A)^* = l_1\ddot{\theta}_1 \cos\theta_1 - l_1\dot{\theta}_1^2 \sin\theta_1, \tag{3}$$

with the two terms on the right-hand side representing the vertical components of tangential and centripetal acceleration, respectively. Thus, all variations in ($\ddot{z}_K - \ddot{z}_A$) due to the terms including $\dot{l}_1$ and $\ddot{l}_1$ may be considered as experimental errors. Figure 2 gives an example of ($\ddot{z}_K - \ddot{z}_A$) and ($\ddot{z}_K - \ddot{z}_A$)* time histories re-

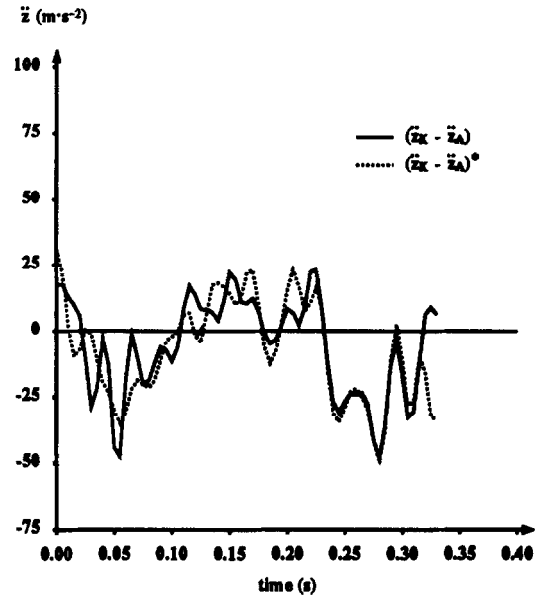

Fig. 2. Time histories of the difference in vertical acceleration between knee and ankle joint of the support leg in heel–toe running. $(\ddot{z}_K - \ddot{z}_A)$ was calculated directly by double differentiation of the positional data, $(\ddot{z}_K - \ddot{z}_A)^*$ was calculated assuming a constant distance between knee and ankle markers [cf. equation (3)]. Curves have been plotted from the last frame before touch-down ($t=0$) to take off.

corded during the support phase in heel–toe running. Differences of up to 25 m s^{-2} occurred during the first 70 ms. These differences are of the order of 25 to 30% of the maximum values reached by $\ddot{z}_K$ and $\ddot{z}_A$. Equations and considerations similar to the ones presented here hold for $(\ddot{z}_H - \ddot{z}_K)$, the difference in the vertical accelerations of the hip and knee joint markers.

Kinetic analysis

The intersegmental forces and moments were calculated using an inverse dynamics approach. The required locations (and accelerations) of the segmental mass centers were estimated from marker positions (and accelerations) using the data presented by Clauser *et al.* (1969) on locations of segmental mass centers as percentages of segment lengths. Segmental masses were estimated using the total body mass and the data reported by Clauser *et al.* (1969) on segmental masses as percentages of the body mass. Transverse segmental moments of inertia were estimated using the estimates of the previous segmental properties in combination with the values reported by Plagenhoeff *et al.* (1983) on segmental radii of gyration as percentages of the length from the joint centers of rotation.

It should be mentioned here that in an inverse dynamics approach, accurate calculation of the net intersegmental forces and moments requires accurate calculation of the contributions of segments to the ground reaction force. For instance, the net force between upper leg and lower leg is obtained by subtracting from the measured ground reaction force the calculated force contributions of foot and lower leg. If the calculated acceleration peaks of these segments were too low, because of errors involved in the method of calculating accelerations of segmental mass centers by double differentiation of marker position time histories, the net intersegmental force and moment at the knee joint would be overestimated. As mentioned before, circumstantial evidence that the method followed for collecting and processing the positional data yields good estimates of segmental accelerations was provided by Bobbert *et al.* (1991); they showed that the first peak in $F_z(t)$ measured using a force plate could be calculated from the positional data with errors of less than 10%.

RESULTS AND DISCUSSION

Kinematics and forces

Except when explicitly mentioned otherwise, the results presented and discussed were extracted from the trials in which the subjects used their preferred running speed and style. The running speeds selected in these trials ranged from 3.8 to 4.5 m s^{-1}. All three subjects were so-called rearfoot strikers (Cavanagh and LaFortune, 1980) or heel–toe runners (Nigg *et al.*, 1988), producing 'impact force peaks' in F_z that ranged from 1400 to 1850 N. Although the results varied somewhat from trial to trial and from subject to subject, the overall pattern of kinematic and kinetic changes was the same across trials and subjects. This

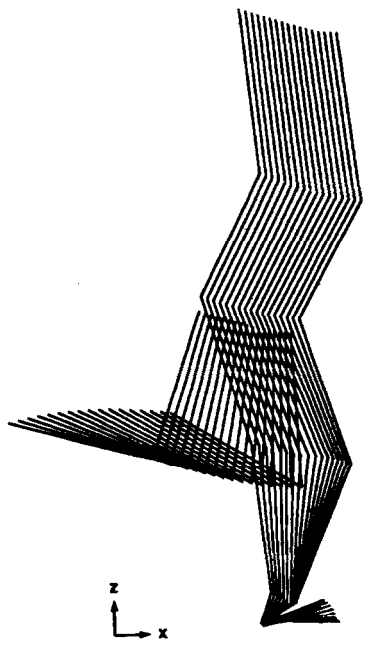

Fig. 3. Stick figures for the first part of the contact phase in heel–toe running. The leftmost stick figure shows the segment orientations on the last frame before touch-down. Time between two subsequent stick figures is 5 ms.

overall pattern will be described and discussed using the results of a single trial. It should be stressed here that if any of the other trials had been selected, the outcome would have been qualitatively identical, although quantitatively slightly different. Figure 3 presents stick figures for the phase of interest in this trial, starting on the last frame before touch-down ($t=0$). For clarity, the stick figures have been separated and the swing leg has been deleted to show velocity vectors of markers at support leg ankle, support leg knee, support leg hip, sternum and head (Fig. 4), acceleration vectors of these markers (Fig. 5), and a free-body

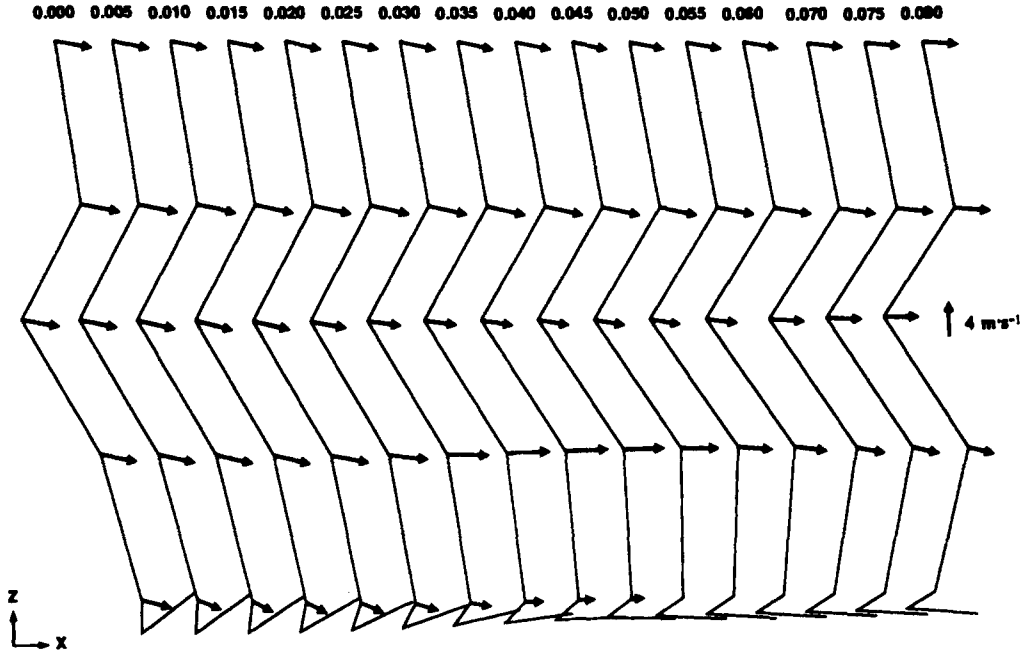

Fig. 4. Velocity vectors of markers at support leg ankle, support leg knee, support leg hip, sternum and head. For clarity, the stick figures have been separated and the swing leg has been deleted. The leftmost stick figure ($t=0$) shows the situation on the last frame before touch-down. Time between two subsequent stick figures is 5 ms.

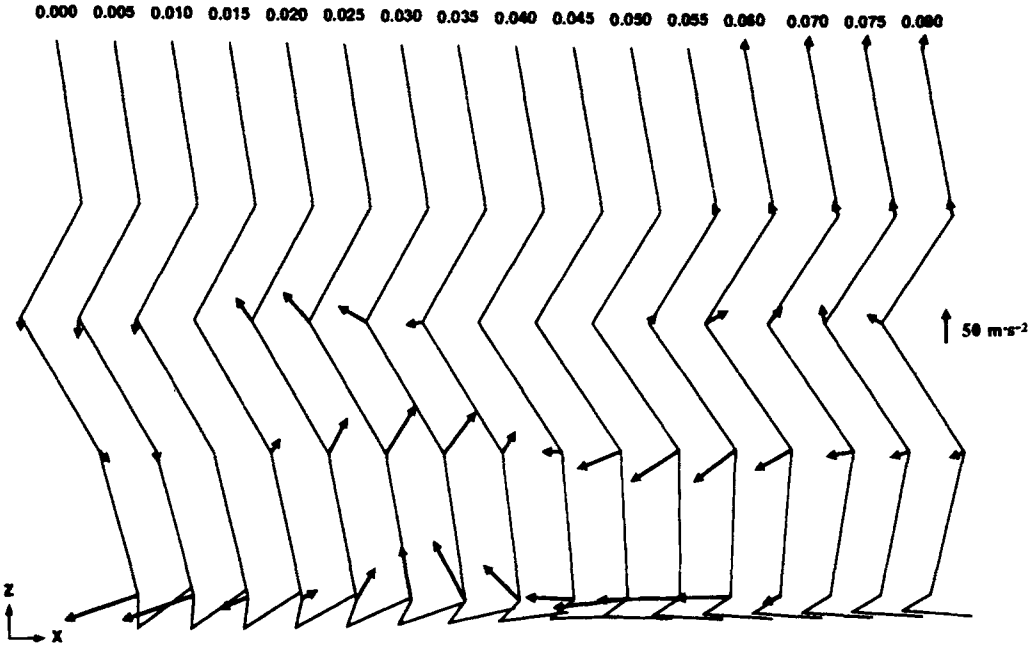

Fig. 5. Acceleration vectors of markers at support leg ankle, support leg knee, support leg hip, sternum and head. For clarity, the stick figures have been separated and the swing leg has been deleted. The leftmost stick figure ($t=0$) shows the situation on the last frame before touch-down. Time between two subsequent stick figures is 5 ms.

diagram of the whole body (Fig. 6); note that in the first two stick figures after touch-down in Fig. 6, the ground reaction force vector is too small to be plotted. In the remaining part of this paper, the swing leg will no longer be considered; unless specified otherwise, designations such as 'lower leg' and 'knee joint' refer to components of the support leg.

Since running is concerned with moving forward, an interesting variable to consider is the horizontal velocity. While the velocity of the foot is rapidly reduced to zero, the horizontal velocities of head and sternum markers, which reflect the horizontal velocity of the heavy mass of HAT, remain almost constant (Fig. 4). In this particular trial, the horizontal velocity of the head marker changed from 4.4 $m\,s^{-1}$ at touch-down to 4.2 $m\,s^{-1}$ during the support phase, and back to 4.4 $m\,s^{-1}$ at take-off, a variation of less than 5%. This value is typical for the variation observed in the other trials in which the subjects used their preferred speed and style. The variations in the horizontal component of the ground reaction force (Fig. 6) are associated primarily with horizontal accelerations of the support leg segments, which have a relatively low mass. Note, for instance, that in the phase where the horizontal component of the ground reaction force vector is large (between $t=0.04$ s and $t=0.060$ s, Figs 6 and 10), the horizontal components of the net joint reaction force at the hip joint are close to zero (Fig. 10). This is the phase where the foot comes flat on the force plate and large horizontal accelerations occur at the knee and ankle joints (Fig. 5).

The relationship between kinematics and variations in the vertical component of the ground reaction force vector is more complex, because the vertical velocity of the large mass of HAT does change considerably. The vertical velocity of the markers on head and sternum was reduced from $-1.0\,m\,s^{-1}$ at touch-down to $-0.4\,m\,s^{-1}$ at $t=0.080$ s. Figure 6 shows that during this phase the vertical component of the ground reaction force vector increases to reach a first peak at $t=0.025$ s (the 'impact force peak'), decreases to a local minimum reached at $t=0.040$ s and, thereafter, increases again. The calculated and the measured $F_z(t)$ curves, and contributions of body segments to the calculated $F_z(t)$ curve, are shown in Fig. 7. As discussed in a previous paper (Bobbert *et al.*, 1991), the first peak in $F_z(t)$ has its origin in upward acceleration of the support leg segments. Its magnitude, however, is determined to a large extent by the contribution of the rest of the body. This is due to its large mass rather than to high vertical accelerations; in Fig. 5, where all marker acceleration vectors are plotted on the same scale, the ones pertaining to head and sternum markers do not even appear until $t=0.055$ s. Note that acceleration vectors do appear for the hip joint marker. Differences between these vectors and vectors for sternum and head markers were found to occur in some parts of the landing phase because of rotational motion in the frontal plane of the pelvis about the support leg hip joint, causing the mass center of HAT to be displaced (accelerated) relative to this joint.

In Fig. 5 it can also be seen that when the sole of the

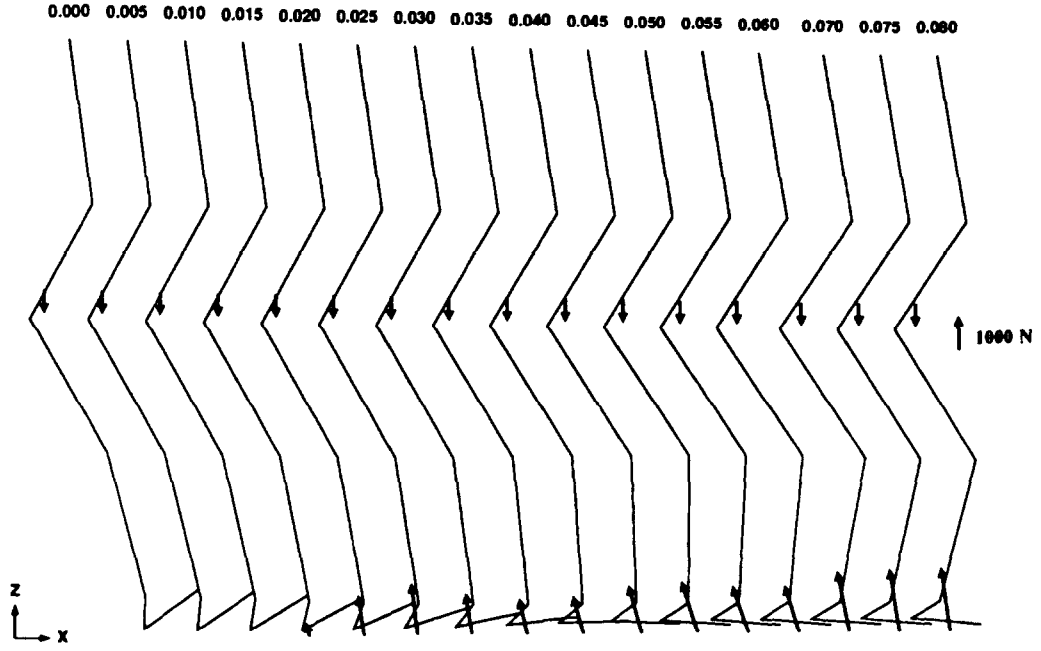

Fig. 6. Free-body diagrams showing the vector of the ground reaction force and the vector of the force of gravity. For clarity, diagrams have been separated and the swing leg has been deleted. The leftmost figure ($t=0$) shows the situation on the last frame before touch-down. Time between two subsequent diagrams is 5 ms.

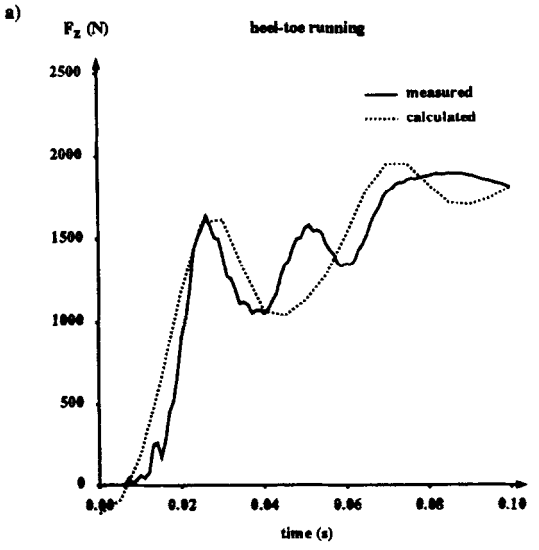

Fig. 7. (a) Calculated and measured time histories of the vertical ground reaction force (F_z). (b) Segmental contributions to $F_z(t)$. Curves have been plotted from the last frame before touch-down ($t=0$). The mass of the subject was 71 kg.

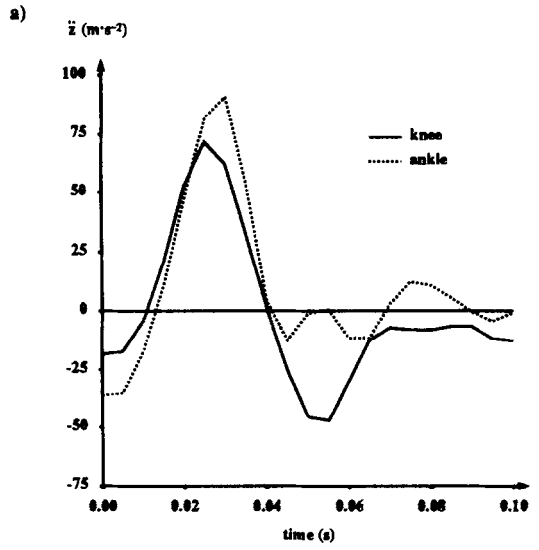

Fig. 8. (a) Time histories of the vertical accelerations of knee and ankle joint markers in the support leg ($\ddot{z}_K$ and $\ddot{z}_A$, respectively). (b) Time histories of the vertical acceleration difference $(\ddot{z}_K - \ddot{z}_A)^*$ calculated according to equation (3), and the contributions to $(\ddot{z}_K - \ddot{z}_A)^*$ of centripetal acceleration $(l_1\dot{\theta}_1^2 \sin\theta_1)$ and tangential acceleration $(l_1\ddot{\theta}_1 \cos\theta_1)$ of the lower leg [cf. equation (3)]. Curves have been plotted from the last frame before touch-down ($t=0$).

shoe becomes horizontal, the direction of the acceleration vector of the knee joint marker changes from upward to downward. Thus, the downward velocity of the shank no longer decreases but begins to increase. This is a consequence of the fact that the ankle joint can no longer move forward. Since the forward velocity of the knee joint is maintained, motion of the lower leg is limited to rotation about the now stationary ankle joint. This rotation is associated with a centripetal acceleration pointing from the knee to the ankle, with the negative acceleration being relatively large because the lower leg is almost vertical. Similar results have been reported by LaFortune and Hennig, 1989). The change in the direction of the acceleration vector of the knee joint marker from upward to downward is accompanied by a reduction of the upward acceleration of the hip joint marker (vectors in Fig. 5 disappear between $t=0.04$ s and $t=0.05$ s), which corresponds in time to the phase where $F_z(t)$ goes through a local minimum (Fig. 6).

The observations presented above were subjected to a quantitative analysis. Figure 8 shows the time histories of the vertical accelerations of the knee and the ankle joint markers ($\ddot{z}_K$ and $\ddot{z}_A$, respectively), the vertical acceleration difference $(\ddot{z}_K - \ddot{z}_A)^*$ calculated according to equation (3), and the contributions to $(\ddot{z}_K - \ddot{z}_A)^*$ of centripetal and tangential accelerations of the lower leg [cf. equation (3)]. It has already been pointed out that $(\ddot{z}_K - \ddot{z}_A)^*$ gives a better impres-

sion of these contributions than $(\ddot{z}_K - \ddot{z}_A)$ calculated directly by double differentiation of the positional data. It turns out that $(\ddot{z}_K - \ddot{z}_A)^*$ is almost zero during the phase where the first peak occurs in $F_z(t)$. After $t = 0.035$ s, the vertical component of *centripetal* acceleration helps to reduce $\ddot{z}_K$ relative to $\ddot{z}_A$. The contribution of centripetal acceleration to $(\ddot{z}_K - \ddot{z}_A)^*$ peaks at $t = 0.055$ s, just after the ankle joint has experienced its maximum backward acceleration (Fig. 5) and its horizontal velocity has become very small. The results of a similar analysis of the contribution of rotation of the upper leg to the vertical acceleration difference between hip and knee joints, $(\ddot{z}_H - \ddot{z}_K)^*$, are presented in Fig. 9. In this case, the most important contribution comes from the vertical component of the *tangential* acceleration of the upper leg. Because of this component, $\ddot{z}_H$ is lower than $\ddot{z}_K$ during the first 40 ms of the support phase, and $\ddot{z}_H$ remains positive in spite of the fact that $\ddot{z}_K$ is negative between $t = 0.045$ s and $t = 0.075$ s.

One of the purposes of this study was to determine the role of segmental rotations in limiting the forces that occur during the landing phase. In order to fully appreciate this role in limiting the vertical forces, it should be realized that rotation of a support leg segment affects not only the vertical acceleration of the mass center of that particular segment but also the vertical acceleration of segments proximal to it. Since most of the mass of the body is located proximal to the hip joint, the influence of rotation of a support leg segment on $F_z(t)$ is determined primarily by its effect on $\ddot{z}_H$. Looking at the results from this point of view, it becomes clear that if rotation of the upper leg had not occurred during the first 40 ms of the support phase, $\ddot{z}_H$ would have been higher (up to a maximum of $\pm 50\ \mathrm{m\,s^{-2}}$), $\ddot{z}_{HAT}$ would have been higher, and the first force peak in $F_z(t)$ would have been higher (theoretically up to a maximum of ± 3000 N). Thus, it may be said that rotation of the upper leg, because of the associated tangential acceleration, plays a major role in limiting F_z during the first 40 ms of the support phase. In a similar way it may be argued that rotation of the lower leg, because of the associated centripetal acceleration, also plays a role in limiting F_z between $t = 0.040$ s and $t = 0.100$ s. In this phase it acts opposite to the clockwise angular acceleration of the thigh, which, as it slows down the anticlockwise angular velocity, tends increase the value of F_z.

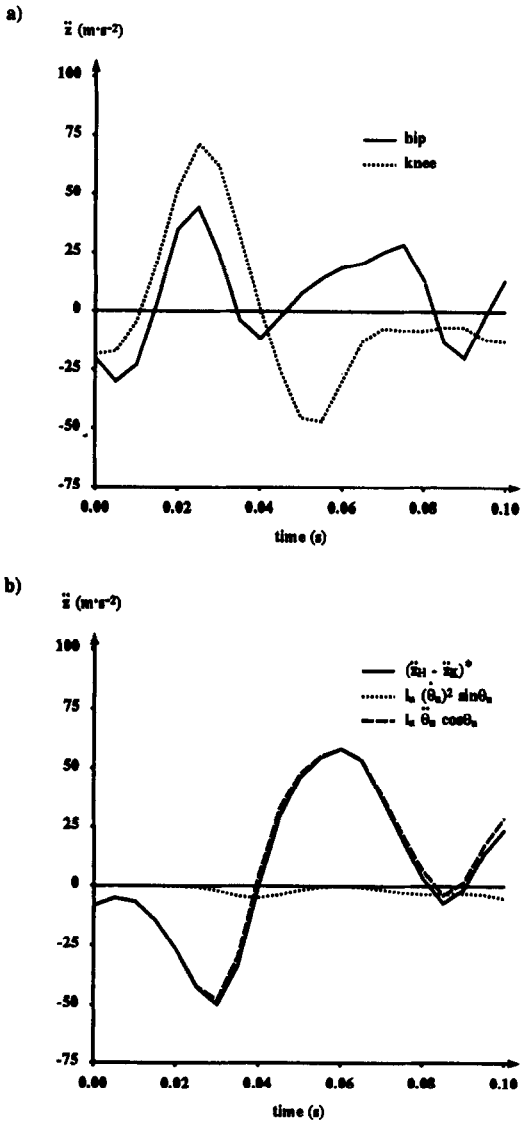

Fig. 9. (a) Time histories of the vertical accelerations of hip and knee joint markers in the support leg ($\ddot{z}_H$ and $\ddot{z}_K$, respectively). (b) Time histories of the vertical acceleration difference $(\ddot{z}_H - \ddot{z}_K)^*$, and the contributions to $(\ddot{z}_H - \ddot{z}_K)^*$ of centripetal acceleration $(l_u \dot{\theta}_u^2 \sin\theta_u)$ and tangential acceleration $(l_u \ddot{\theta}_u \cos\theta_u)$ of the upper leg. Curves have been plotted from the last frame before touch-down ($t = 0$).

Kinematics and moments

Figure 10 shows the free-body diagrams of the upper leg and the lower leg for the first 80 ms of ground contact. For the sake of clarity in illustration, intersegmental moments have been shown as circular arrows, with the center of the circle lying at the proximal or distal end of a segment and the angle of the arc corresponding to the magnitude of the moment; a circular arrow pointing anticlockwise represents a moment vector coming out of the paper. In the landing phase, the limits of the ranges of motion in hip, knee and ankle joints are not approached. Thus, the moments exerted by passive structures about these joints will be small, and it seems safe to interpret changes in the net intersegmental moments about these joints as changes in the net muscle moments.

Before touch-down hip extension and knee flexion moments are present, indicating a backward acceleration of the leg segments relative to the rest of the body. This explains why the acceleration of the ankle joint is backward (Fig. 5) although there is no ground reaction force yet (Fig. 6). The moment about the hip joint does not change direction, although it decreases

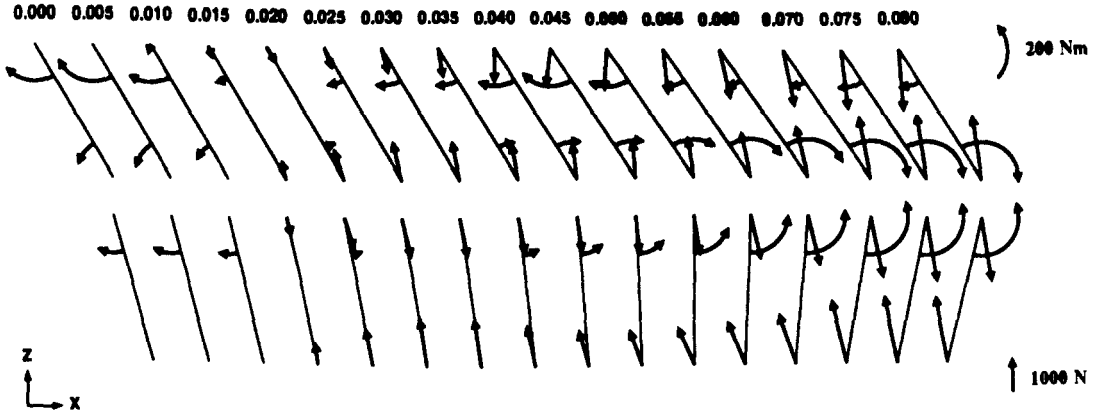

Fig. 10. Free-body diagrams of support upper leg and lower leg. Proximal and distal intersegmental forces have been shown as vectors with their origin at the segmental endpoints, proximal and distal intersegmental moments have been shown as circular arrows, with the center of the circle lying at a segmental end point and the angle of the arc corresponding to the magnitude of the moment; a circular arrow pointing anticlockwise actually represents a moment vector coming out of the paper. For clarity, the diagrams have been separated and the swing leg has been deleted. The leftmost figure ($t=0$) shows the situation on the last frame before touch-down. Time between two subsequent diagrams is 5 ms.

temporarily during the phase where the knee joint is accelerated downward, i.e. between $t=0.040$ s and $t=0.070$ s (Fig. 10). The moment about the knee joint, however, does change direction; it switches from flexion to extension between touch-down and $t=0.035$ s. At the instant where the first peak in $F_z(t)$ occurs, the proximal and distal joint reaction forces acting on the tibia are directed along the long axis of the lower leg, and the knee joint moment is almost zero. The same phenomenon was found in trials where the subjects used other-than-preferred running styles, including Groucho running (running while keeping the body's mass center low, as described by McMahon *et al.* (1987). Between $t=0.030$ s and $t=0.055$ s, the knee extension moment increases from 10 to 200 Nm. At the ankle joint, a dorsiflexion moment occurs during the first 45 ms of ground contact; this may be concluded from the fact that the ground reaction force vector passes posterior of the joint (Fig. 6). The moment values are, however, too small to be plotted on the same scale as the moments about knee and hip joints; the maximum dorsiflexing moment is only 24 Nm. This value is typical of all running trials of the three subjects. Note that during the first 15 ms, $\ddot{z}_A$ remains downward (Fig. 8), indicating that the moments exerted about the ankle have little effect on the movement.

Neuromuscular control during the landing phase

One of the most interesting questions is whether neuromuscular control *during* the landing phase in running has any influence on the forces occurring in this phase. Figure 10 shows that changes in the net moments about the joints occur, but since these changes are extremely rapid it is unlikely that they are due to changes in the muscle activation levels. Let us consider, for instance, the change from -100 Nm (flexion) to $+200$ Nm (extension) which occurs in the net moment about the knee joint during the first 55 ms of ground contact (these values are typical of the trials in which the subjects used their preferred running speed and style). If a subject is instructed to contract his knee extensor muscles as rapidly and forcefully as possible while the knee angle is kept constant in a dynamometer, it typically takes more than 100 ms before the knee extension moment has increased from 0 to 100 Nm (see e.g. Viitasalo *et al.*, 1980; Viitasalo, 1982). Moreover, significant changes in the moments due to stretch reflexes do not seem to occur within the first 100 ms after stretch (Melvill Jones and Watt, 1971; Gottlieb and Agarwal, 1979a, b). In order to explain the rapid changes in the moment about the knee joint during running that were observed in this study, the following hypothesis may be put forward. At touch-down, co-contraction of knee extensor and knee flexor muscles is present, with the knee flexors exerting a larger moment than the knee extensors (since a net knee flexing moment is present at touch-down). Because of the collision with the ground, a rapid knee flexion occurs so that the knee flexors experience a quick release, causing the force exerted by them to drop. Simultaneously, the knee extensors experience a sudden stretch, which causes the force produced by them to increase. Both the decrease in the force exerted by the knee flexors and the increase in the force produced by the knee extensors contribute to a rapid change in the net moment about the knee joint from flexion to extension.

The mechanism proposed above assumes spring-like behavior of muscle–tendon complexes during rapid changes in the distance between origin and insertion. The stiffness of muscle–tendon complexes under such conditions varies with the stiffness of the cross-bridge array, which, in turn, depends on the number of cross bridges (Morgan, 1977). Since the changes in the net knee joint moment are relatively large, with a flexion moment of 100 Nm being close to the maximum isometric knee flexion moment (Wickie-

wicz et al., 1984) and an extension moment of 200 Nm possibly even exceeding the maximum isometric knee extension moment (Wickiewicz et al., 1984), we need a strong co-contraction of knee extensor and knee flexor muscles and a concomitant high stiffness for the proposed mechanism to work. Results of electromyographic studies suggest that a strong co-activation of quadriceps femoris and hamstring muscles does occur before touch-down and during the first part of the support phase in running (Elliott and Blanksby, 1979; Mann and Hagy, 1980; Mann et al., 1986). It has been speculated that this co-activation serves the purpose of lower limb stabilization (Elliott and Blanksby, 1979). According to the argument given above, however, co-activation is an essential step in the preparation for the landing phase. Without it, the rate of change of muscle moments about the knee joint would depend on the rate of force development (or decay) following changes in muscle activation. This rate is relatively low because of the interaction between contractile elements and series elastic elements, and possibly also because the active state of muscles may rise or decay slower than the level of muscle activation (Bobbert and van Ingen Schenau, 1990). Thus, the absence of co-activation could lead to a loss of (passive) control of body motion during the landing phase.

Touch-down conditions and segmental force contributions during landing

In the previous paragraph it was shown that during the first 25 ms of the landing phase, where $F_z(t)$ increases to reach its first peak, lower leg rotation does not reduce $\ddot{z}_K$ relative to $\ddot{z}_A$. Thus, the acceleration of the mass centre of the lower leg and, therewith, the contribution of the lower leg to $F_z(t)$, depends purely on what happens distal to the ankle joint. It was also shown that $\ddot{z}_A$ does not become positive until $t=0.015$ s, while the moment arm of the ground reaction force vector with respect to the ankle joint remains close to zero during the impact phase, at least in the sagittal plane projection (Fig. 6). It seems, therefore, that the ankle dorsiflexor muscles have little influence on $\ddot{z}_A$, so that the collision of the lower leg (and foot) with the force plate should be comparable to a mass striking a spring, the spring being formed by the elastic structures underneath the calcaneus (calcaneal fat pad and sole of the shoe). In the case of a mass striking a spring, the force developed during the collision increases with the initial velocity, the absolute force level depending on the spring stiffness (McMahon et al., 1987). Figure 11(a) shows for one subject (the one who performed 20 running trials) the contribution of the lower leg to the first peak in $F_z(t)$ (Fig. 7) as a function of $|\dot{z}_{A,max}|$, the maximal downward velocity of the ankle joint (in the case of the trial used for illustration, $|\dot{z}_{A,max}|$ was reached at $t=0.015$ s). The coefficient of linear correlation between the two was 0.82 ($p<0.01$). Figure 11(b) shows for the same trials the contribution of the upper leg to the first peak in $F_z(t)$ (Fig. 7) as a function of $|\dot{z}_{A,max}|$. Again, a high correlation of 0.77 ($p<0.01$) was found. The latter finding is not really surprising; $\ddot{z}_K$ equals $\ddot{z}_A$ when the first peak in $F_z(t)$ occurs, and $\ddot{z}_K$ determines approximately half the vertical acceleration of the mass centre of the upper leg. It seems that the collision of the support leg with the ground can indeed be described as a collision between a mass and a spring. A similar description was proposed earlier by Denoth

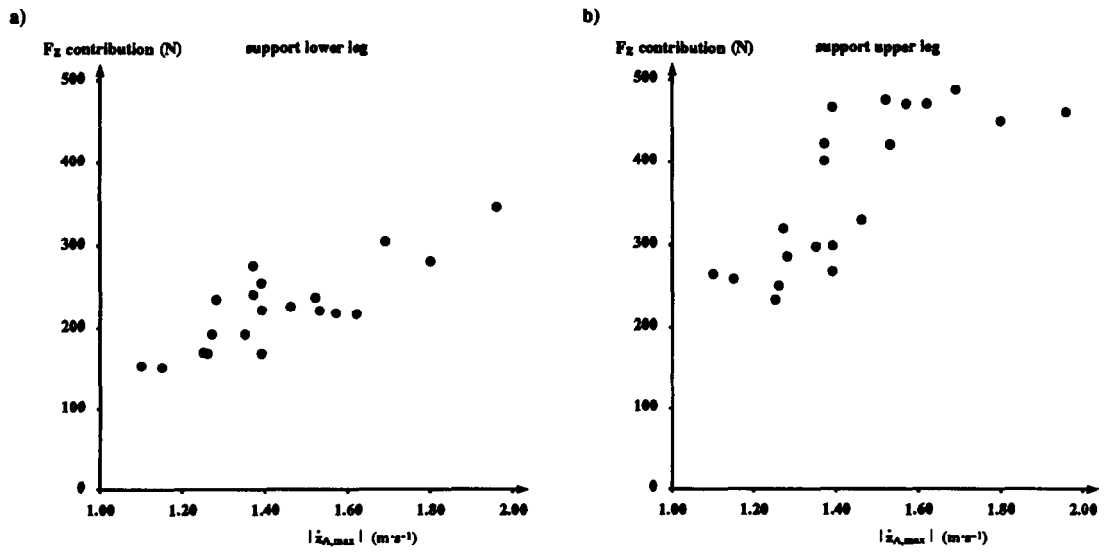

Fig. 11. (a) Contribution of the support lower leg to the first peak in $F_z(t)$ (Fig. 7) plotted as a function of $|\dot{z}_{A,max}|$, the maximal downward velocity of the ankle joint. (b) Contribution of the support upper leg to the first peak in $F_z(t)$ (Fig. 7) plotted as a function of $|\dot{z}_{A,max}|$. Each data point represents the results of one trial, with all trials belonging to one subject.

(1986) and Nigg and Morlock (1987). Since the spring stiffness depends on the stiffness of the shoe sole and the stiffness of the surface, it is theoretically possible to reduce the force contributions of the upper and the lower legs to the first peak in $F_z(t)$, and therewith attenuate the high-frequency force peaks 'seen' by the knee and ankle joints. Whether this is a practical solution or not depends, of course, on how thick the shoe sole or surface would have to be for that. As pointed out in a previous study (Bobbert *et al.*, 1991), the effects of changes in shoe or surface stiffness on forces occurring during the impact phase should be evaluated by determining the segmental contributions to the first peak in $F_z(t)$ and not by determining only the absolute value of this peak. The reason is that the segmental force contributions of support leg segments and the rest of the body (Fig. 7) can be varied independently. In this context, it is relevant to mention that the coefficient of linear correlation between the first peak in $F_z(t)$ and $|\dot{z}_{A,max}|$ was only 0.5.

Final remarks and future research

Based on a mechanical analysis of running trials of three subjects, it was argued in this paper that during the first 25 ms of the landing phase in heel–toe running, where F_z increases to reach its first peak, changes in muscle moments about the joints are so rapid that they have to be caused by spring-like behavior of pre-activated muscles. This implies that the runners investigated had no opportunity to control the rotations of body segments during this period, other than by selecting the initial conditions, i.e. by selecting a certain geometry of the body and muscular (co-) activation levels prior to touch-down. It would be interesting to know the criteria used in selecting the initial conditions. One of them seems to be that the backward acceleration of HAT is minimized during landing, so that a minimal amount of energy is utilized for re-increasing the horizontal velocity of HAT. In the vertical direction, the situation is less clear. For energy requirements it may be useful to minimize the vertical excursion of HAT, so that no energy is wasted in moving up and down. However, this requires high vertical accelerations of HAT, leading to large forces and possibly hazardous loads on the locomotor system. It is noteworthy that selecting an almost vertical position of the lower leg at touch-down, rather than a position past vertical, at the same time allows for limitation of the vertical acceleration of HAT (because the contribution of centripetal acceleration helps to reduce $\ddot{z}_K$ relative to $\ddot{z}_A$) *and* keeps the vertical excursion of HAT small ($z_K - z_A$ is actually slightly increased during the first 50 ms of ground contact, as can be seen in Fig. 4). Although selecting this position of the lower leg at touch-down seems advantageous for controlling the motion HAT, it also seems to be partly responsible for the occurrence of the high-frequency force peak in $F_z(t)$. Our understanding of the selection of initial conditions may be improved by studying what would happen to the mechanics of the landing phase if the position of the lower leg or pre-activation levels of muscles were changed. Possibly, such changes, which could occur when runners become fatigued, are involved in the development of injuries. For a study of the effects of the intial conditions on the mechanics of the landing phase, forward dynamics simulation of the landing phase in heel–toe running with a mathematical model of the musculoskeletal system seems indicated.

Acknowledgements—This study was supported by grant #8345 of the Alberta Heritage Foundation for Medical Research, and by grant #OGPIN-001 from the Natural Sciences and Engineering Research Council of Canada.

REFERENCES

Bobbert, M. F. and Schamhardt, H. C. (1990) Accuracy of determining the point of force application with piezoelectric force plates. *J. Biomechanics* **23**, 705–710.

Bobbert, M. F., Schamhardt, H. C. and Nigg, B. M. (1991) Calculation of vertical ground reaction force estimates during running from positional data. *J. Biomechanics* **24**, 1095–1105.

Bobbert, M. F. and van Ingen Schenau, G. J. (1990) Isokinetic plantar flexion: experimental results and model calculations. *J. Biomechanics* **23**, 105–119.

Cavanagh, P. R. and LaFortune, M. A. (1980) Ground reaction forces in distance running. *J. Biomechanics* **13**, 397–406.

Clauser, C. E., McConville, J. T. and Young, J. W. (1969) Weight, volume and center of mass of segments of the human body. AMRL-TR-69-70, pp. 59–60. Wright-Patterson Air Force Base, OH.

Denoth, J. (1986) Load on the locomotor system and modelling. In *Biomechanics of Running Shoes* (Edited by Nigg, B. M.), pp. 63–116. Human Kinetics Publishers, Champaign, IL.

Elliott, B. C. and Blanksby, B. A. (1979) The synchronization of muscle activity and body segment movements during a running cycle. *Med. Sci. Sports Exercise* **11**, 323–327.

Frederick, E. C., Hagy, J. L. and Mann, R. A. (1981) Prediction of vertical impact force during running. *J. Biomechanics* **14**, 498 (abstract).

Gottlieb, G. L. and Agarwal, G. C. (1979a) Response to sudden torques about ankle in man: myotatic reflex. *J. Neurophysiol.* **41**, 91–106.

Gottlieb, G. L. and Agarwal, G. C. (1979b) Response to sudden torques about ankle in man: postmyotatic reactions. *J. Neurophysiol.* **43**, 86–100.

Hinrichs, R. N., Cavanagh, P. R. and Williams, K. R. (1987) Upper extremity function in running. I. Center of mass and propulsion considerations. *Int. J. Sports Biomech.* **3**, 222–241.

Kistler (1984) *Multicomponent Measuring Force Plate for Biomechanics and Industry Type 9287.* Kistler Instrumente AG, Winterthur.

Komi, P. V., Gollhofer, A., Schmidtbleicher, D. and Frick, U. (1987) Interaction between man and shoe in running: considerations for a more comprehensive measurement approach. *Int. J. Sports Med.* **8**, 196–202.

LaFortune, M. A. and Hennig, E. M. (1989) Contribution of angular motion and gravity to tibial acceleration. In *Proceedings of the XIIth International Congress of Biomechanics*, abstract #334. University of California, Los Angeles.

Lees, A. and McCullagh, P. J. (1984) A preliminary investigation into the shock absorbency of running shoes and shoe inserts. *J. Hum. Mvmt Stud.* **10**, 95–106.

Mann, R. A. and Hagy, J. (1980) Biomechanics of walking, running and sprinting. *Am. J. Sports Med.* **8**, 345–350

Mann, R. A., Moran, G. T. and Dougherty, S. E. (1986) Comparative electromyography of the lower extremity in jogging, running and sprinting. *Am. J. Sports Med.* **14**, 501–510.

McMahon, T. A., Valiant, G. and Frederick, E. C. (1987) Groucho running. *J. appl. Physiol.* **62**, 2326–2337.

Melvill Jones, G. and Watt, D. G. D. (1971) Observations on the control of stepping and hopping movements in man. *J. Physiol.* **219**, 709–727.

Morgan, D. L. (1977) Separation of active and passive components of short-range stiffness of muscle. *Am. J. Physiol.* **232**, C45–C49.

Nigg, B. M., Bahlsen, H. A., Luethi, S. M. and Stokes, S. (1987) The influence of running velocity and midsole hardness on external impact forces in heel–toe running. *J. Biomechanics* **20**, 951–959.

Nigg, B. M., Herzog, W. and Read, L. J. (1988) Effect of viscoelastic shoe soles on vertical impact forces in heel–toe running. *Am. J. Sports Med.* **16**, 70–76.

Nigg, B. M. and Morlock, M. (1987) The influence of lateral heel flare of running shoes on pronation and impact forces. *Med. Sci. Sports Exercise* **19**, 295–302.

Plagenhoeff, S., Evans, F. G. and Abdelnour, T. (1983) Anatomical data for analysing human motion. *Res. Quart. Exercise Sport* **54**, 169–178.

Viitasalo, J. T. (1982) Effects of pretension on isometric force production. *Int. J. Sports Med.* **3**, 149–152.

Viitasalo, J. T., Saukkonen, S. and Komi, P. V. (1980) Reproducibility of measurements of selected neuromuscular performance variables in man. *Electromyogr. clin. Neurophysiol.* **20**, 487–501.

Wickiewicz, T. L., Roy, R. R., Powell, P. L., Perrine, J. and Edgerton, V. R. (1984) Muscle architecture and force–velocity relationships in humans. *J. Appl. Physiol. Respirat. Environ. Exercise Physiol.* **57**, 435–443.